Hindawi
Advances in Civil Engineering
Volume 2019, Article ID 5090326, 10 pages
https://doi.org/10.1155/2019/5090326

Research Article

Mechanism of Secondary Breakage in the Overlying Strata during Repetitious Mining of an Ultrathick Coal Seam in Design Stage

Hui Li,[1,2] Dongsheng Zhang,[1] Shuyin Jiang,[1] Gangwei Fan,[1,3] and Mengtang Xu[4]

[1]*State Key Laboratory of Coal Resources and Safe Mining, China University of Mining & Technology, Xuzhou 221116, China*
[2]*Xinjiang Branch of China National Coal Group Corp., Urumqi 830011, China*
[3]*School of Mines, China University of Mining & Technology, Xuzhou 221116, China*
[4]*School of Mining Engineering, Guizhou Institute of Technology, Guiyang 550003, China*

Correspondence should be addressed to Dongsheng Zhang; dshzhang123@126.com

Received 20 September 2018; Revised 12 December 2018; Accepted 6 January 2019; Published 3 February 2019

Academic Editor: Humberto Varum

When designing the mining of an ultrathick coal seam, the laws governing movement in the overlying strata during mining are a fundamental issue based on which several problems are addressed, including determining the mining method and the roadway arrangement, controlling the surrounding strata, and selecting the devices. The present paper considers possible problems related to strata overlying a large mining space subjected to repeated disturbances during the mining of an ultrathick coal seam, including repeatedly broken strata and the existence or inexistence of the structure. The B_M coal seam in the No. 2 coal mine of the Dajing mining area in the East Junggar coalfield is studied. Physical simulations are performed on the movements of the overlying strata during slicing mining of the ultrathick coal seam, revealing the new feature of "break-joint stability-instability-secondary breakage" in the overlying strata. Mechanical models are constructed of the secondary breakage of the overlying strata blocks under both static and impact loading, and mechanical criteria are proposed for such breakage. Based on the research findings, methods for controlling the surrounding strata during slicing mining of an ultrathick coal seam are proposed, including increasing the mining rate and designing reasonable heights for the slicing mining.

1. Introduction

The mining areas of Western China have abundant coal resources. In the autonomous region of Xinjiang in particular, the predicted coal stock is 1,820–2,190 billion tons, which is 40.5% of the total predicted coal stock and ranks first in China. An important feature of the coal resources in Xinjiang is the wide distribution of ultrathick coal seams (UTCSs). For instance, all the coalfields in the Ili, Tuha, and Cubey regions with predicted coal stocks greater than 10 billion tons have UTCSs in which the thickness of a single layer exceeds 20 m. Moreover, in the East Junggar coalfield, which is the largest integrated coalfield in the world, a single layer can be as thick as 80 m and the average thickness is 43 m. The average thickness in the No. 2 coal mine in the Zhaotong coalfield exceeds 50 m, with single layers up to 193 m thick. In the Gippsland Basin of Southeast Australia, the total thickness of the coalfield can be as much as 700 m, with single layers around 230 m thick. Finally, the maximum total thickness of the Kazakhstan River coalfield in Canada is 510 m. The above information shows that UTCSs are widely distributed around the world [1–3]. However, UTCSs with single layers as thick as 40 m have only been mined in open-pit mines both in China and elsewhere in the world. For underground mines, the current technique of fully mechanized caving mining has a maximum mining height of 20 m. However, UTCSs with a thickness of 40 m inevitably require the use of slicing mining (SM), thereby presenting the problem of how to control the stability of the overlying strata (OS) when mining a UTCS with a large mining space and repeated mining disturbances [4, 5].

Both in China and internationally, there has been much theoretical and practical research regarding the laws governing the movement of OS in mining [6–8]. In Germany,

Holla and Bulzen used cantilever theory to explain the periodic weighting that occurs in the stope [9], and Sirivardane proposed a compressive-arch theory aimed at the support pressure in the strata surrounding the working face [10]. In Belgium, Labasse used a model involving a beam with preformed cracks to reveal the mechanism for the formation of preformed cracks in a coal seam and its roof [11]. Yao et al. and Wood investigated (i) the mining conditions required for the formation of OS affected by mining and (ii) the mechanical conditions required for cracks to form in the separation layer of the OS [12, 13]. Qian and Li established a mechanical model of a voussoir-beam structure and proposed a discriminant method for dealing with destabilization in the articulated structure of OS blocks [14]. Wu et al. studied the features of OS subsidence in repetitious mining and derived an equation with which to calculate the subsidence coefficient inside the rock mass under such conditions [15].

The above research was focused mainly on thick coal seams, namely, those that are 3.5–20 m thick; research remains scarce regarding mining UTCSs, namely, those whose thickness exceeds 20 m. Moreover, all current theories about how OS move assume that they break only once [16–21]. Rotary instability and sliding instability are two modes of instability during roof weighting of coal seams with normal thicknesses [22–24]. However, compared to coal seams with normal thickness, the strata structures of UTCSs vary considerably during the mining process. As a UTCS is mined, the goaf space increases considerably, resulting in a larger space for movement of OS in the stope. In particular, UTCSs under SM suffer frequent disturbances, a wide range affected by mining, and a large intensity of mining, thereby causing more-complicated movements of the OS blocks and obvious changes in the three-zone structure. The caving zone becomes increasingly tall and can even reach the ground surface, thereby causing a large-scale instability break in the OS structures and posing a severe threat to safe production in mines [25–28].

From the above discussion, the movement of the OS during SM of a UTCS requires further research. But in the history and current situation of UTCS mining worldwide, there has been only the case of mining UTCS (40 m) through open-pit mining. For underground coal mining, the maximum mining thickness is about 20 m, and the number of slices does not exceed 3. The engineering practice and theoretical research of underground UTCS mining are still at the exploratory stage, and there is very little to draw from. Besides, No. 2 coal mine in the Dajing mining area, the studied area of this paper, is currently at the initial stage of mining design. No mining plan or SM scheme has been formulated yet. To achieve scientific mining of the B_M coal seam (40 m thick), key issues such as SM scheme, roadway arrangement, surrounding rock control, and equipment selection must be solved. And to attain these goals, it is necessary to understand overlying strata movement and the underlying mechanism in the mining process of UTCS through basic tests. Therefore, this paper tries to provide answers to the following two questions: first, compared to a normal coal seam, what are the new features of the movements in the OS in a UTCS subjected to repetitious mining? Second, why do OS blocks break repeatedly in a UTCS subjected to repetitious mining? To answer these questions, taking the B_M coal seam in the No. 2 coal mine of the Dajing mining area in the East Junggar coalfield as the studied target area, we (i) explore features of the fractures in the OS during mining, (ii) establish a mechanical model of the OS structure during mining, and (iii) analyze the mechanism whereby the OS move during mining. This lays a foundation for controlling the stability of the rocks surrounding the working face in a UTCS.

2. Geological Conditions of Studied Area

The B_M coal seam in the No. 2 coal mine of the Dajing mining area in the East Junggar coalfield, which is a typical UTCS in the Xinjiang region, was selected for study herein. This coal mine is a 10-million-ton mine developed and constructed by the Xinjiang Fukang Energy Development Co., Ltd. It is located 140 km north of Qitai County and is around 13 km long from south to north, around 12 km long from east to west, and occupies an area of 155.8 km^2. The mine has coal reserves of 10,469.7 Mt and a production capacity of 15 Mt/y. The primarily mined B_M coal seam has an average thickness of 44 m, a tilt angle of 1–3°, and a local tilt angle of 6°. The B_M coal seam has a stable occurrence, a simple structure including 0–5 layers of tonstein and developed fractures. The primary lithology of the OS with a fluvial swamp face deposit is light-gray and gray mudstone as well as silty mudstone. The OS contain UTCSs and sandstone layers. The immediate roof has an average thickness of 6.6 m and a lithology of gritstone and fine sandstone. The main roof has an average thickness of 9.5 m and a lithology of fine sandstone. There is a layer of fine-granule conglomerate, primarily quartziferous gravel, at the bottom of the coal seam, which changes gradually into fine sandstone when moving toward the basin center along the inclination. The coal seam and underlying Sangonghe formation strata present generally conformable contact and contact scouring locally. No. 2 coal mining of Dajing mining area is currently at the initial stage of mining design, and no mining plan has been developed yet. Figure 1 and Table 1 show a composite histogram of the mine and the mechanical performance parameters of the strata, respectively.

3. Physical Simulation Experiments of Mining an Ultrathick Coal Seam

To understand the basic features of OS movement in the mining process of UTCS and to determine the general rules of breakage of OS, physical simulation experiments were conducted on SM of the B_M coal seam. As a widely used and effective means to study OS movement, the physical simulation experiment can realistically and intuitively reflect OS movement, and it is especially fit for the movement and breakage morphology of a certain stratum or OS block. Its superiority over other research methodologies has already been established. Several physical simulation experiments were carried out in this study, and the purpose of which was

Erathem	System	Series	Group	Code	Thickness (m)	Columnar 1 : 200	Lithology	Description	Maker beds
Cenozoic erathem	Quaternary system	Holocene series	Alluvial-proluvial sand grains	$Q_{3\text{-}4}^{al+pl}$	40	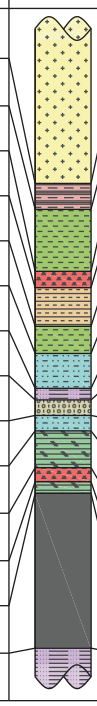	Weathered sandstone	Wide distribution and uneven thickness	
	Tertiary system	Pliocene series	Dushanzi group	N_2^d	6.7		Sandstone	Gray, current bedding	
Mesozoic erathem	Cretaceous system	Lower series	Tugulu group	K_1^{tg}	16		Interbedded mudstone-sandstone	Local average thickness of 16 m	
	Jurassic system	Upper-middle series	Shishugou group $J_{2\text{-}3}^{sh}$	Upper subgroup $J_{2\text{-}3}^{sh^a}$	4.2		Gritstone	Local average thickness of 4.2 m	
					10		Mudstone	Light gray, current bedding	
					7		Interbedded mudstone-sandstone	Local average thickness of 7 m	
				Lower subgroup $J_{2\text{-}3}^{sh^b}$	9		Sandy mudstone	Light brown, current bedding	
					3		Siltstone	Light gray, stratiform	
					4		Medium sandstone	Light gray, massive joint	
		Middle series	Xishanyao group	J_2^x	4		Sandy mudstone	Light brown, current bedding	
					9.5		Fine sandstone	Gray, current bedding	Main roof
					3.6		Gritstone	Local average thickness of 3.6 m	Immediate roof
		Lower series	Sangonghe group	J_1^s	3		Fine sandstone	Gray, current bedding	
					44		Coal seam	Bright coal, dull coal	B_M Coal seam
					4.3		Siltstone	Light gray, stratiform	Immediate floor

Figure 1: Composite histogram of the no. 2 coal mine.

Table 1: Mechanical performance parameters of overlying strata (OS) in the B_M coal seam.

No.	Lithology	Thickness (m)	Elasticity modulus (GPa)	Density (10^3 kg·m^{-3})	Compressive strength (MPa)	Cohesion (MPa)	Internal friction angle (°)
#1	Weathered sandstone	40	5.0	1.7	/	0.5	/
#2	Sandstone layer	6.7	10.0	2.3	5	1.1	28
#3	Interbedded mudstone-sandstone	16	16.5	1.9	32.8	8.3	38
#4	Gritstone	4.2	39.7	2.7	54.8	23.6	36.5
#5	Mudstone	10	10.8	1.7	25.7	1.6	38.5
#6	Interbedded mudstone-sandstone	7	17.6	1.9	34.9	12.6	39
#7	Sandy mudstone	9	38	2.5	23	2.5	32
#8	Siltstone	3	16	2.1	39	10.5	35
#9	Medium sandstone	4	19.2	2.5	43.2	14.8	40
#10	Sandy mudstone	4	38	2.5	23	3.5	32
#11	Fine sandstone	9.5	19.2	2.4	50	4.5	40
#12	Gritstone	3.6	42.1	2.7	56.3	23.9	36.5
#13	Fine sandstone	3	35	2.6	56.6	23.1	37.5
#14	Coal	44	13	1.5	18.3	1.54	30

to accurately and qualitatively describe the OS movement features in the mining of UTCS and to lay the basis for the subsequent SM planning of the coal mine.

3.1. Test Model and Scheme. The physical model has layout dimensions of 1.3 m (length) × 0.3 m (width) × 1.2 m (height). The primary similarity coefficients of the model were determined as follows using three similarity theories: a geometry ratio of 1 : 135, a volume-to-weight ratio of 1 : 1.67, a time ratio of 10, and a material-strength similarity ratio of 1 : 225. Boundary coal pillars with a width of 15 cm were set at both sides of the model. The coal seam was mined layer by layer with a mining length of 100 cm, which equates to an actual mining length of 135 m. The mining height of the coal seam was 30 cm, which equates to an actual mining height of 40 m. Figure 2 shows the entire model.

The layer-by-layer mining mode was considered as follows: the coal seam was mined in six layers: the first four of which were each mined by 5 m height, and the remaining two were each mined by 10 m height. The open-off cut of the coal seam was located at the right-hand side of the model.

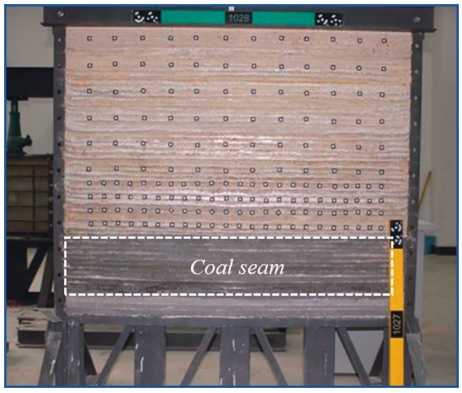

Figure 2: Physical model simulating the mining of an ultrathick coal seam (UTCS).

The working face was mined from the right to left with a mining length of 4 cm, which equates to an actual mining length of 5.4 m. After completing the mining of each layer and ensuring that the OS were stable, mining began on the next layer with the open-off cut right below that of the layer above. Each layer was actually mined 25 times, and the UTCS model was mined 150 times in total.

3.2. Test Results. Figure 3 shows the process of OS movements during the physical simulation experiments of a coal seam being excavated. The OS movement patterns were clearly the same in the initial SM of the UTCS as in the mining of a coal seam with normal thickness. Obvious phenomena of first weighting and periodic weighting occurred in the #11 fine sandstone (main roof). As shown in Figures 3(a) and 3(b), as the SM of the UTCS progressed, the goaf space increased considerably. If the failed rock mass below the key #11 fine sandstone could support the latter effectively, then the key stratum remained structurally stable during the periodic SM. As shown in Figure 3(c), if the failed rock mass below the #11 fine sandstone could not support the goaf as the number of slices being mined increased, structural instability would occur in the #11 fine sandstone. As shown in insets I and II in Figure 3(c), when the working face on the third slice was driven forward from the open-off cut to 36 m, some parts of the #11 fine sandstone broke again. Following structural instability, two fractures formed in the OS, reaching the ground surface along the direction of the caving angle of the strata on the two sides of the working face. As the SM continued, because of repetitive mining-induced impact, the masses in the #12 and #13 strata near the goaf were in a disordered state (Figure 3(d)). Moreover, as the SM became thicker, the height of the disordered OS increased. In the stoping of the last two slices, some masses of the #11 fine sandstone broke again because of the large mining space and the repeated disturbances caused by the SM, as shown in Figures 3(e) and 3(f). Insets I and II of Figure 3(f) show the free-fall breaking of the masses as the working face was driven forward to 44 m. Taken together, in the SM of the entire UTCS, the #11 fine sandstone as the main roof underwent breakage-hinged stability-instability-secondary breakage (SB) successively. It was easy to find by comparison that the SB of masses in the #11 fine sandstone was divided into two types. One was caused by squeezing the OS under static exposure and hanging of the masses; this type of breakage occurred mainly in the early stage of OS movement during the SM of the UTCS. The other type was related to collision impact during unstable falling of the masses; the latter occurred mainly in the latter stage of OS movement during the SM.

4. Mechanism for Secondary Breakage of Overlying Strata Blocks in an Ultrathick Coal Seam

Based on the results of the physical simulation experiments in Section 3, to reveal in more detail the mechanism for SB in the OS blocks of a UTCS, further research was performed on the SB under the effects of static loading and impact loading from a mechanical perspective.

4.1. Secondary Breakage of Overlying Strata Blocks under Static Loading. According to the research results, the SB of OS blocks under static loading occur mainly in the following situation: after the instability of the hinge structures in the blocks, the blocks present as a cantilever structure (as shown in Figure 4). As the mining of the coal seam proceeds, its hanging length increases and the extent of the underlying strata supporting the blocks reduces, causing a rapid increase in the tension stress suffered by the side walls of the OS blocks. When the maximum tension stress exceeds the limit load, tension breaks occur in the blocks.

Figure 4 shows that the stress and the structure in the mechanical model of the stope is symmetrical, and therefore, only the right-hand half of the model is analyzed. When the OS blocks undergo the cantilever-type SB, both ends are considered as free, and the stress in the OS blocks is considered as a uniformly distributed load q. Therefore, the simplified mechanical model shown in Figure 5 is established.

The model is a statically determinate structure. The bending moment suffered by the blocks is as follows:

$$M = \left(\frac{1}{2}\right) gHx^2, \tag{1}$$

where γ (kN/m^3) is the volume force of the OS and H (m) is the height of the overlying load. The maximum bending moment appears at the left-hand end of a hanging block, where $x = l_x$ with a maximum value of

$$M_{\max} = \left(\frac{1}{2}\right) \gamma H l_x^2, \tag{2}$$

where l_x (m) is the length of the hanging block. From the cantilever-beam calculation, the maximum tension stress $\sigma_{\max}$ is

$$\sigma_{\max} = \frac{6 \times (1/2)\gamma H l_x^2}{h^2} = \frac{3\gamma H l_x^2}{h^2}, \tag{3}$$

where h (m) is the block thickness. When the maximum tensile stress suffered by the block reaches the tensile

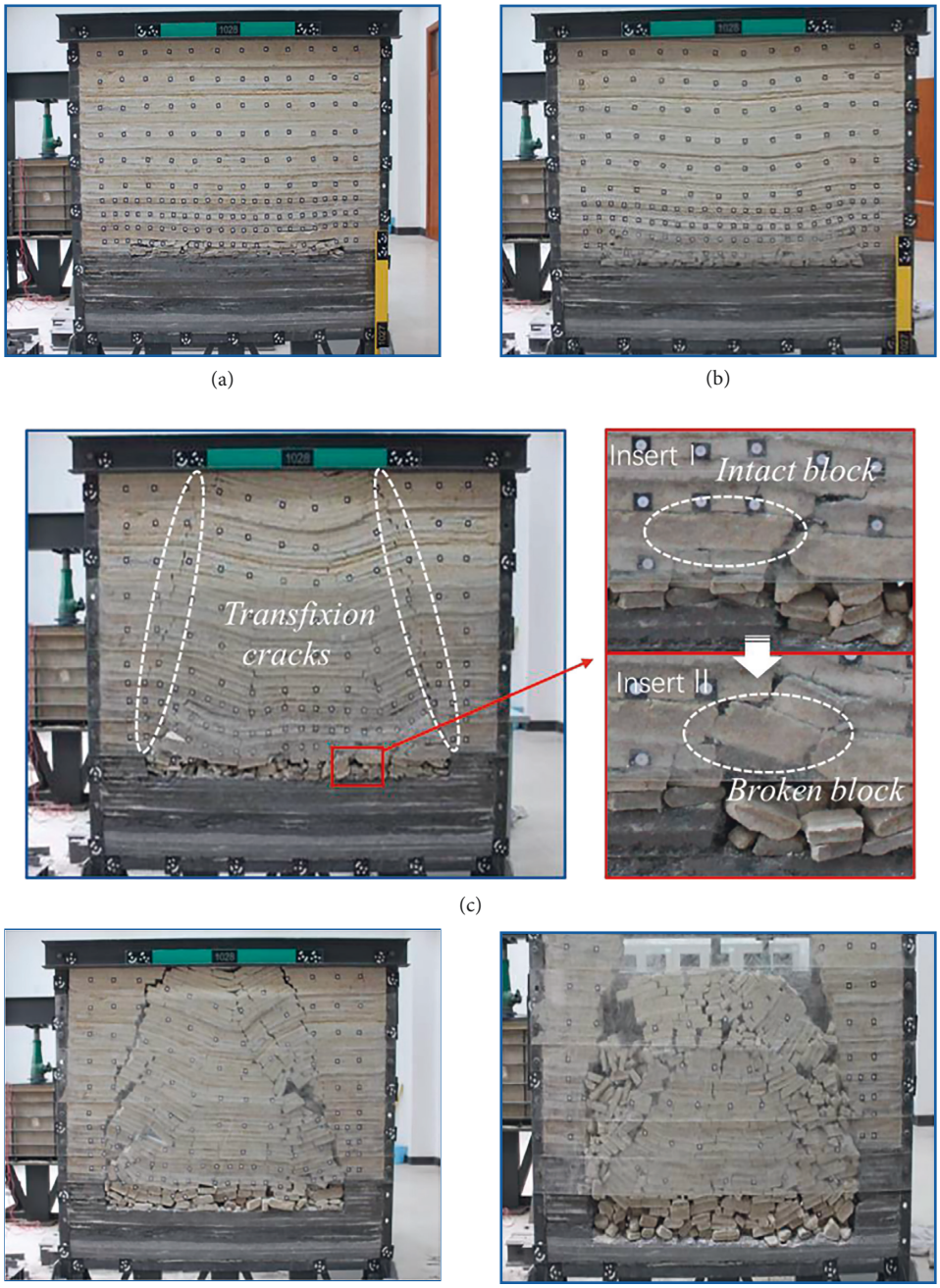

Figure 3: Continued.

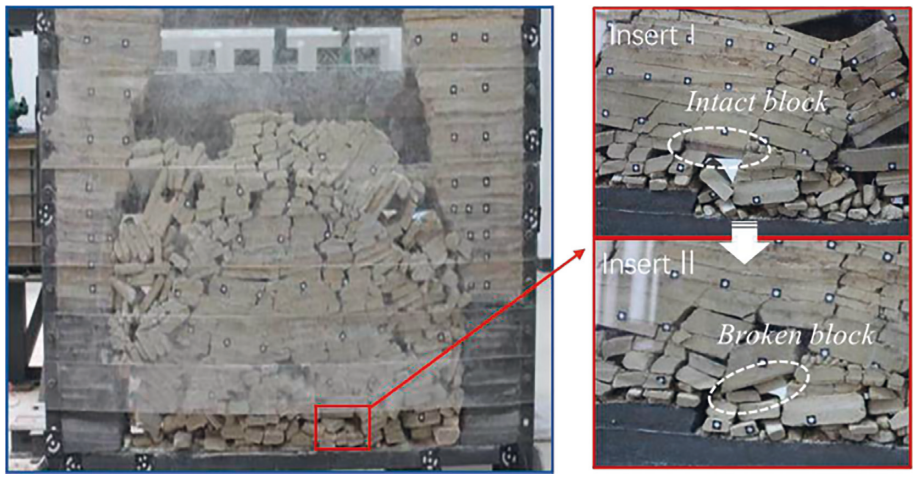

(f)

Figure 3: Structural evolution of overburden when slicing mining (SM) a UTCS: (a) first SM; (b) second SM; (c) third SM; (d) fourth SM; (e) fifth SM; (f) sixth SM.

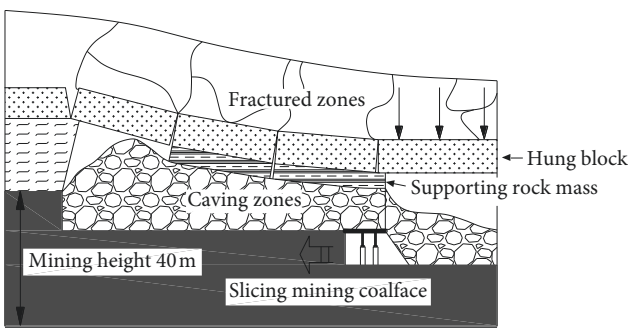

Figure 4: Schematic of the cantilever structure of broken blocks.

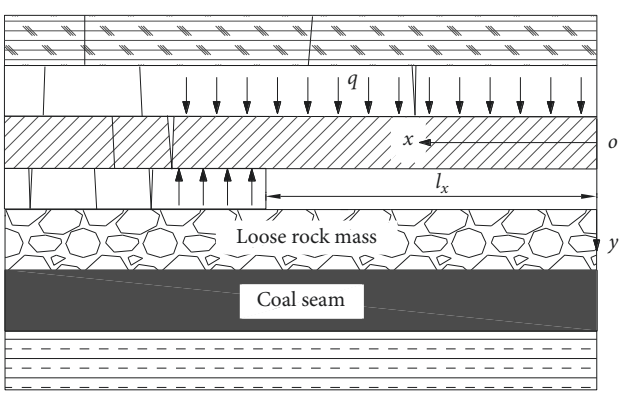

Figure 5: Mechanical model of periodic weighting on key strata.

strength R_T, SB occurs in the OS block, i.e., the discriminant of the SB of a block in the OS under static loading is

$$\frac{3\gamma H l_x^2}{h^2} \geq R_T. \tag{4}$$

4.2. Secondary Breakage of Overlying Strata Blocks under Impact Loading. According to the results of the physical simulation experiments, during the latter stage of SM, there is little variation in the loads acting on the bedrock of broken blocks given that the lengths of the broken blocks have already reached their limit spans. Meanwhile, as the mining space expands longitudinally, the SB of blocks in the OS under impact loading occurs more often during the latter stage of SM.

Figure 3(f) shows that when breaking occurs because of OS blocks falling freely, the adjacent ends of two blocks cannot form a hinged structure; thus, the blocks lack the horizontal constraints of the OS on their left- and right-hand sides. When the working face advances behind the blocks, there is no fulcrum to constrain their ends and thus they fall freely. The process of free-fall block breaking is divided into three main parts: the initial state, the free-fall process, and the collision and breaking process.

4.2.1. Initial State. When a block falls from height h_1, the falling time is so short that the load of the OS is deemed to have always acted on the block, as shown in Figure 6. The initial conditions are initial speed $v_0 = 0$ and acceleration $a = g$.

4.2.2. Free Fall. If the tilt angle of the block is relatively small, each part of the lower surface of the block is deemed to reach the underlying rock mass at the same time, at which time the speed of the block has increased from zero to v_1, as shown in Figure 7. This speed is obtained from the kinetic energy as

$$v_1 = \sqrt{2gh_1}. \tag{5}$$

4.2.3. Collision. After collision, the block continues to move downward, compressing the loose rock mass and therefore decelerating the block. Once the OS and the block are at rest, the loose rock mass is fully compressed with maximum

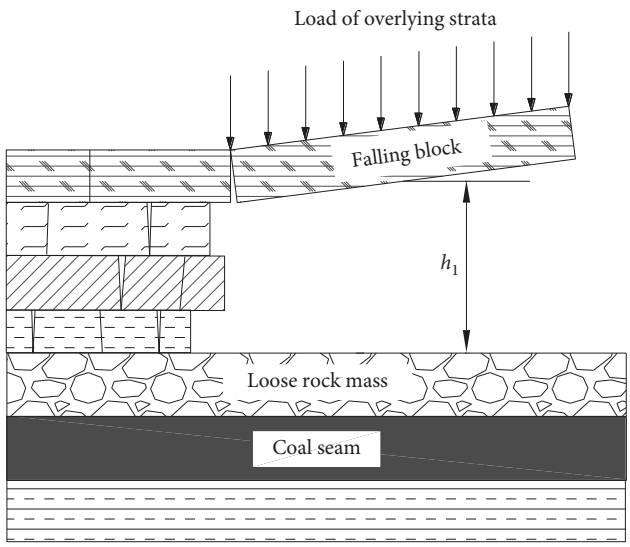

Figure 6: Initial state of the block in free-fall situation.

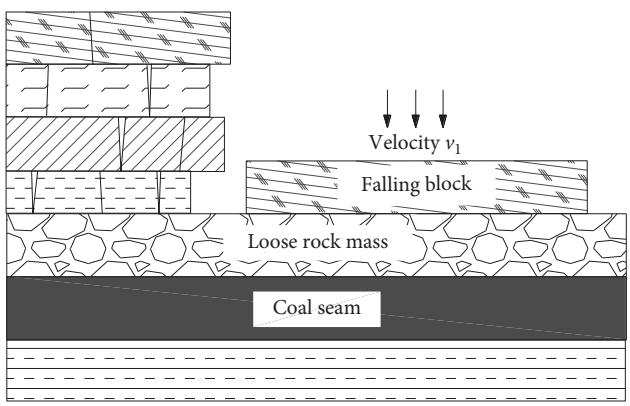

Figure 7: Free-fall process of the block.

compression δ_{max}. Therefore, the loose rock mass can be simplified as a spring, as shown in Figure 8. The elastic coefficient k of the spring is

$$k = \frac{El}{h_2}, \tag{6}$$

where E (MPa) is the average modulus of elasticity of the underlying loose rock mass, l (m) is the length of the falling block, and h_2 (m) is the thickness of the loose rock mass, i.e., the distance from the key stratum to the coal seam.

From collision to maximum compression of the loose layer, the work done by the block's weight is $mg\delta_{max}$ and that done by the restoring force of the loose layer is $-k\delta_{max}^2/2$. At this time, the other blocks in the OS are at rest. It can be obtained from the kinetic energy as follows:

$$0 - \rho(H+h)\left(\frac{lv_1^2}{2}\right) = \rho h \lg \delta_{max} - \left(\frac{k\delta_{max}^2}{2}\right), \tag{7}$$

where ρ (kg/m^3) is the average density of the block, the overlying load layer δ_{max} (m) is the maximum compression of the rock mass, and k is the elastic coefficient of the spring. Then, δ_{max} is calculated as

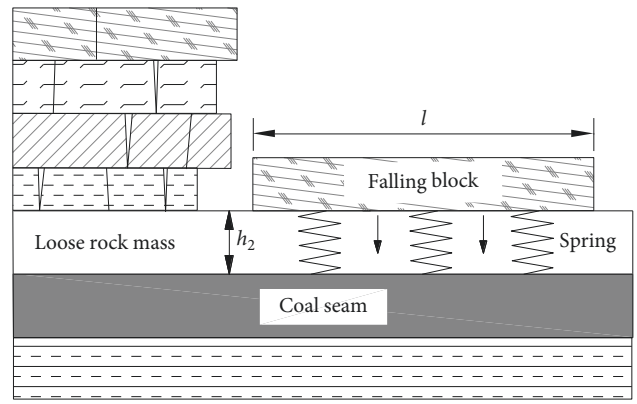

Figure 8: Collision process of the block in the free-fall situation.

$$\delta_{max} = \frac{\rho g h h_2}{E} + \left(\frac{h_2}{El}\right)\sqrt{(\rho g h l)^2 + 2k\rho g l (H+h) h_1}. \tag{8}$$

The maximum restoring force F that the spring provides for the falling block is therefore

$$F = k\delta_{max} = \rho g h l + \sqrt{(\rho g h l)^2 + 2\frac{h_1}{h_2} E\rho g l^2 (H+h)}, \tag{9}$$

and the maximum compression stress σ that the falling block suffers is

$$\sigma = \frac{F}{l} = \rho g h + \sqrt{(\rho g h)^2 + 2\frac{h_1}{h_2} E\rho g (H+h)}. \tag{10}$$

The block is crushed if σ is equal to or greater than σ_c, where σ_c is the compressive strength of the falling block.

5. Discussion

The mechanism for the SB of blocks in an OS under repetitious mining of a UTCS is now basically clear. To obtain relationships between various influential factors and the SB of blocks, the following research was conducted to supplement the research achievements described in Section 4. Given a tensile strength R_T of the rock mass of 5 MPa and an average value of γ of 2.5×10^4 N/m^3, distributions of the stresses suffered by hanging blocks are plotted in Figure 9. Taking a compressive strength $\sigma_c = 30$ MPa for the rock mass, an average density $\rho = 2.5 \times 10^3$ kg/m^3, and an elastic modulus $E = 500$ MPa for the underlying rock mass, the stress of the falling rock mass is plotted in Figure 10 according to equation (9).

From the factors influencing the SB of OS blocks under static loading as shown in Figure 9, block breakage is closely related to lithology, block length, block thickness, and the load of the OS. The maximum tension stress suffered by a block under static loading increases with the length of the hanging block and the load height of the OS but decreases with the block thickness. When the tension stress increases to a certain critical value, the block undergoes SB. Taking a rock mass with a tensile strength $R_T = 5$ MPa as the example, blocks below the critical line in Figure 10 are stable, whereas those above it will break.

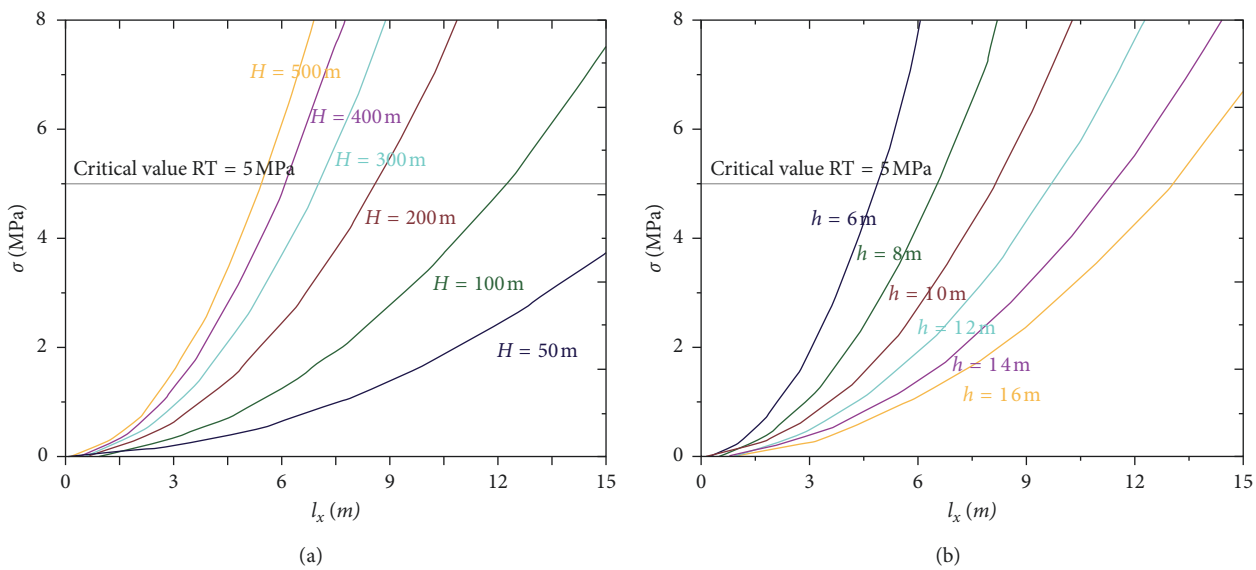

Figure 9: Variation of maximum tensile stress on the hanging block with l_x for different values of H and h: (a) block thickness $h = 15$ m; (b) load height $H = 100$ m.

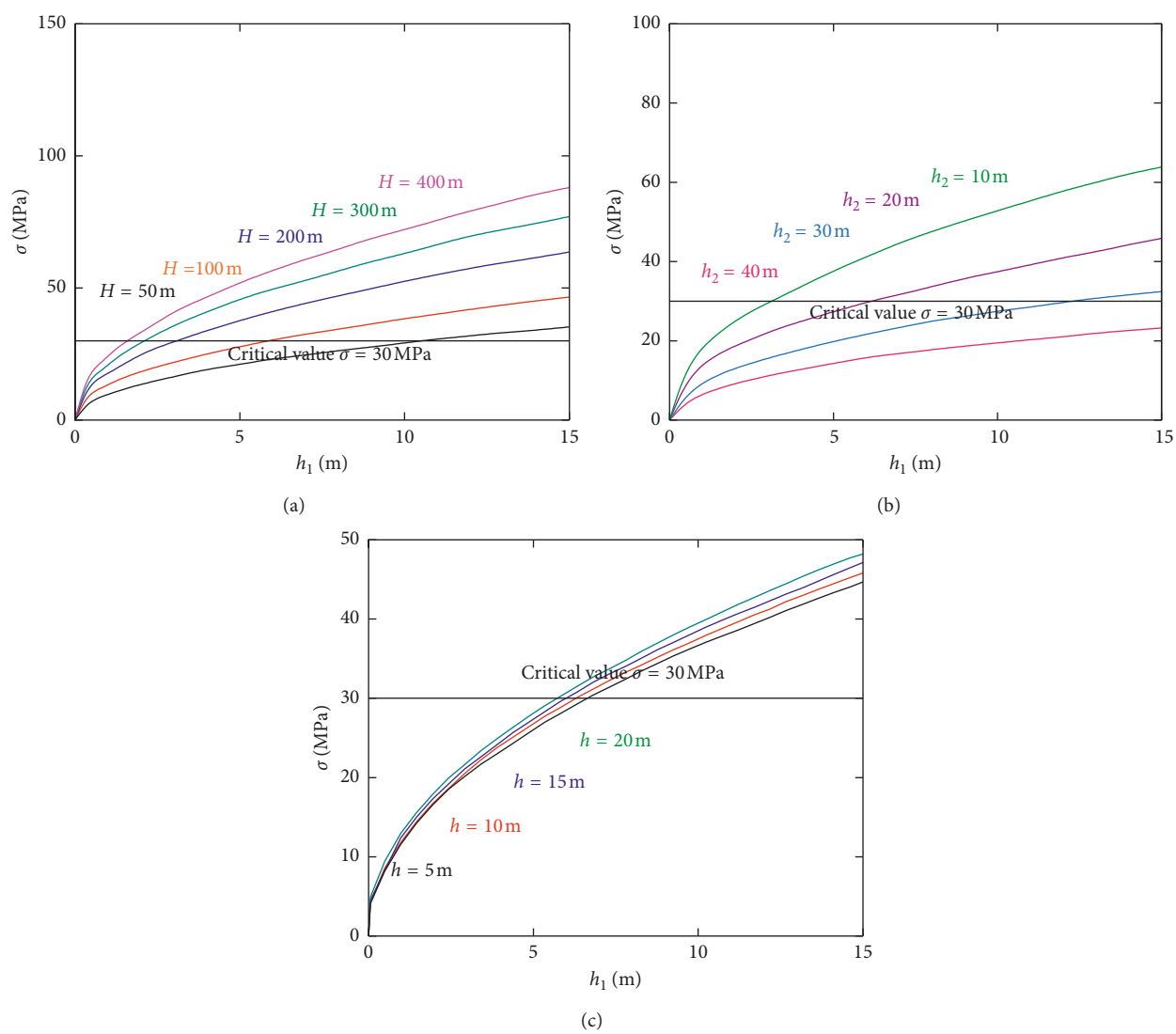

Figure 10: Variation of maximum tensile stress on the hanging block with h_1 for different values of H, h_2, and h: (a) variation of maximum tensile stress on the hanging block with h_1 for different values of H; (b) variation of maximum tensile stress on the hanging block with h_1 for different values of h_2; (c) variation of maximum tensile stress on the hanging block with h_1 for different values of h.

From the factors influencing the free-fall breaking of blocks as shown in Figure 10, the maximum compressive stress suffered by a block when falling and colliding increases with the fall height of the block and the load in the OS, decreases with the thickness of the underlying broken-expanded rock mass, and is little affected by the thickness and length of the block. When the compressive stress increases to a certain critical value, the block undergoes SB. Taking a rock mass with a compressive strength $\sigma_C = 30$ MPa as the example, blocks below the critical line are stable, whereas those above it will break.

Actually, when mining a UTCS, most of the OS blocks experience SB simultaneously under both static and impact loading and even cyclic SB under either alternating static and impact loading or repeated impact loading. However, the key to controlling the stability of the OS lies in guaranteeing that there will be no SB in the blocks therein. Building on the present research results, accelerating the mining appropriately during the actual production process could reduce the hanging length of the OS blocks to a certain extent, thereby lessening the tendency for blocks to undergo SB and enhancing the stability of the surrounding rocks. A typical coalfield in Xinjiang was studied herein to conduct a preliminary exploration of the mechanical mechanism for SB in the OS. Therefore, assessing the validity of the present research results will require a field survey in the East Junggar coalfield in subsequent SM. When designing new mines intended for SM, other than the gradual accumulation of experience, measures such as (i) reducing the height of the upper layer and increasing the height of the lower layer in SM, (ii) recording roof dynamic loads, and (iii) gathering data about the support load in the mining stope could offer enhanced control of the stability of the surrounding rocks during SM of UTCSs.

6. Conclusion

The present aims are possible problems of the OS with a large mining space subjected to repeated disturbances during the mining of a UTCS, including repeatedly broken strata and the existence or inexistence of the structure. Taking the B_M coal seam in the No. 2 coal mine of the Dajing mining area in the East Junggar coalfield as the studied target area, physical simulations were performed to discern the laws governing the movements of the OS when mining a UTCS. Features of the dynamic changes in the OS of a UTCS under repeated mining disturbances were presented, and two basic forms of the SB of blocks were concluded along with their primary features. To reveal the mechanical nature of SB and to investigate general laws for it, mechanical models were constructed of OS blocks undergoing SB subject to either static or impact loading, and mechanical criteria were obtained for the SB of those blocks. The research reported shows that, under static loading, the SB of the OS blocks involves tensile fracture of a cantilever structure once the blocks become unstable. It is easier for SB to occur in OS blocks with longer hanging length, shorter height, and higher load from the OS. Under impact loading, SB of the OS blocks occurs mainly because of kinetic energy released from the OS during the collision process. The key factors that control whether SB occurs in the OS blocks under impact loading are (i) the fall height, (ii) the load of the OS, and (iii) the thickness of the underlying broken-expanded rock mass.

Data Availability

No data were used to support this study.

Conflicts of Interest

The authors declare that there no conflicts of interest.

Authors' Contributions

Hui Li and Dongsheng Zhang did conceptualization. Gangwei Fan was responsible for the methodology. Hui Li, Gangwei Fan, and Mengtang Xu performed physical experiments. Hui Li and Dongsheng Zhang did mechanical analysis. Mengtang Xu managed resources. Hui Li, Dongsheng Zhang, and Gangwei Fan cured the data. Dongsheng Zhang authorised the paper.

Acknowledgments

This work was supported by the National Basic Research Program (grant no. 2015CB251600) and the National Natural Science Foundation of China (grant no. 51264035).

References

[1] M. T. Xu, W. Zhang, X. F. H. L. Liu, W. M. Guan, and R. Zhou, "Study on overburden strata movement law seam and working resistance above near vertical super-thick of powered support," *Coal Science and Technology*, vol. 45, no. 5, pp. 76–79, 2017.

[2] G. S. Li, Q. Zeng, L. H. Zhao, and P. Gao, "Simulation of the impact of super-thick coal seam mining on overlying aquifers: a case study of Dajing mining area of Eastern Junggar coalfield," *China Mining Magazine*, vol. 27, no. 3, pp. 104-105, 2018.

[3] M. T. Xu, "Study on movement laws of overlying strata and its control of ultra-thick coal seam mining in Xinjiang region," Dissertation, China University of Mining and Technology, Xuzhou, China, 2014.

[4] J. Guo, G. Feng, P. Wang, T. Qi, X. Zhang, and Y. Yan, "Strata behavior and support resistance determination for ultra-thick longwall top coal caving panel: a case study of the tashan coal mine," *Energies*, vol. 11, no. 5, pp. 1041–1043, 2018.

[5] X. Deng, J. Zhang, T. Kang, and X. Han, "Strata behavior in extra-thick coal seam mining with upward slicing backfilling technology," *International Journal of Mining Science and Technology*, vol. 26, no. 4, pp. 587–592, 2016.

[6] M. Karmis, T. Triplett, C. Haycocks, and G. Goodman, "Mining subsidence and its prediction in the Appalachian coalfield," in *Proceedings of 24th U.S. Symposium on Rock Mechanics*, College Station, TX, USA, June 1983.

[7] C. C. He and J. L. Xu, "Subsidence prediction of overburden strata and surface based on the voussoir beam structure theory," *Advances in Civil Engineering*, vol. 2018, Article ID 2606108, 13 pages, 2018.

[8] V. Palchik, "Formation of fractured zones in overburden due to longwall mining," *Environmental Geology*, vol. 44, no. 1, pp. 28–38, 2003.

[9] L. Holla and M. Bulzen, "Strata movement due to shallow longwall mining and the effect on ground permeability," *Aus IMM Bulletin and Proceedings*, vol. 295, no. 1, pp. 175–181, 1990.

[10] A. Sirivardane, "Displacement based approach for prediction of subsidence cause by long wall mining using numerical method," *Thinconf on Compute Method*, vol. 42, no. 1, pp. 10–21, 1991.

[11] Z. Q. Song, *Practical Method of Mine Pressure Control*, China University of Mining and Technology Press, Xuzhou, China, 3rd edition, 1988.

[12] X. L. Yao, D. J. Reddish, and B. N. Whittaker, "Non-linear finite element analysis of surface subsidence arising from inclined seam extraction," *International Journal of Rock Mechanics and Mining Sciences & Geomechanics Abstracts*, vol. 30, no. 4, pp. 431–441, 1993.

[13] Wood, "Larnach drum constitutive modeling and finite element analysis of ground subsidence due to mining," Dissertation, University of Oklahoma, Norman, OK, USA, 1990.

[14] M. G. Qian and H. C. Li, "The movement of overlying strata in longwall mining and its effect on ground pressure," *Journal of China Coal Society*, vol. 1, no. 2, pp. 1–8, 1982.

[15] K. Wu, Y. H. Wang, and K. Z. Deng, "Application of dynamic mechanics model of overlying strata movement and damage above goaf," *Journal of China University of Mining & Technology*, vol. 29, no. 1, pp. 34–37, 2000.

[16] M. Tsesarsky, "Deformation mechanisms and stability analysis of undermined sedimentary rocks in the shallow subsurface," *Engineering Geology*, vol. 133-134, no. 4, pp. 16–29, 2012.

[17] G. W. Fan, D. S. Zhang, and L. Q. Ma, "Overburden movement and fracture distribution induced by longwall mining of the shallow coal seam in the Shendong coalfield," *Journal of China University of Mining & Technology*, vol. 40, no. 2, pp. 196–201, 2011.

[18] Y. Chen, S. Ma, and Y. Yu, "Stability control of underground roadways subjected to stresses caused by extraction of a 10-m-Thick coal seam: a case study," *Rock Mechanics and Rock Engineering*, vol. 50, no. 9, pp. 2511–2520, 2017.

[19] B. Hu, "Study on strata movement control of twice strip mining," *Advanced Materials Research*, vol. 962-965, pp. 1085–1090, 2014.

[20] M. Rezaei, "Development of an intelligent model to estimate the height of caving-fracturing zone over the longwall gobs," *Neural Computing and Applications*, vol. 30, no. 7, pp. 2145–2158, 2016.

[21] V. Palchik, "Bulking factors and extents of caved zones in weathered overburden of shallow abandoned underground workings," *International Journal of Rock Mechanics and Mining Sciences*, vol. 79, pp. 227–240, 2015.

[22] D. Zhang, G. Fan, L. Ma, and X. Wang, "Aquifer protection during longwall mining of shallow coal seams: a case study in the Shendong Coalfield of China," *International Journal of Coal Geology*, vol. 86, no. 2, pp. 190–196, 2011.

[23] A. Sainoki and H. S. Mitri, "Dynamic behaviour of mining-induced fault slip," *International Journal of Rock Mechanics and Mining Sciences*, vol. 66, pp. 19–29, 2014.

[24] S. Wang, X. Li, and S. Wang, "Separation and fracturing in overlying strata disturbed by longwall mining in a mineral deposit seam," *Engineering Geology*, vol. 226, pp. 257–266, 2017.

[25] X. F. Lv, H. Y. Zhou, A. W. Wang, C. Feng, and X. C. Xiao, "Characteristics of stress transfer and progressive fracture in overlying strata due to mining-induced disturbances," *Advances in Civil Engineering*, vol. 2018, Article ID 8967010, 13 pages, 2018.

[26] Y. Chen, F. G. Gong, and M. Zhao, "The study on the movement law of overlying strata in fully mechanized caving face under alluvium with huge thickness in deep mine," *Iop Conference Series: Earth & Environmental Science*, vol. 59, no. 1, pp. 1–6, 2017.

[27] W. Wang, Y. P. Cheng, H. F. Wang et al., "Fracture failure analysis of hard-thick sandstone roof and its controlling effect on gas emission in underground ultra-thick coal extraction," *Engineering Failure Analysis*, vol. 54, no. 5, pp. 151–160, 2015.

[28] C. Li, X. K. Sun, J. H. Xu, and Q. L. Chang, "Slicing filling principle and repeated mining key technology for extra-thick coal seams in small coalpit destroyed areas," *Bulgarian Chemical Communications*, vol. 49, no. 1, pp. 66–70, 2017.